Synthesis of WO_3/Pt Nanoparticle by Microwave-assisted Sol-gel Method for Enhanced Photocatalytic Property in Visible Light

Widiyandari, Hendri
Department of Physics, Faculty of Mathematics and Natural Science, Universitas Sebelas Maret

Ayash, Yahya
Department of Physics, Faculty of Science and Mathematics, Universitas Diponegoro

Muhammad Shalahuddin Al Ja' farawy
Department of Physics, Faculty of Mathematics and Natural Science, Universitas Sebelas Maret

Subagio, Agus
Department of Physics, Faculty of Science and Mathematics, Universitas Diponegoro

他

https://doi.org/10.5109/6781060

出版情報：Evergreen. 10 (1), pp.139-145, 2023-03. 九州大学グリーンテクノロジー研究教育センター
バージョン：

Synthesis of WO_3/Pt Nanoparticle by Microwave-assisted Sol-gel Method for Enhanced Photocatalytic Property in Visible Light

Hendri Widiyandari[1,4*], Yahya Ayash[2], Muhammad Shalahuddin Al Ja'farawy[1], Agus Subagio[2], Wahyu Bambang Widayatno[3]

[1]Department of Physics, Faculty of Mathematics and Natural Science, Universitas Sebelas Maret, Indonesia

[2]Department of Physics, Faculty of Science and Mathematics, Universitas Diponegoro, Indonesia

[3]Research Center for Physics, National Research and Innovation Agency (BRIN), Indonesia

[4]Centre of Excellence for Electrical Energy Storage Technology, Universitas Sebelas Maret, Indonesia

*Author to whom correspondence should be addressed:
E-mail: hendriwidiyandari@staff.uns.ac.id

(Received October 14, 2022; Revised January 22, 2023; accepted February 6, 2023).

Abstract: Pt co-catalyst WO_3 (WO_3/Pt) nanoparticle has been synthesized with a variation of platinum co-catalyst mass percentage using the microwave-assisted sol-gel method. The XRD characterization results show that WO_3/Pt has a triclinic (anorthic) crystal structure. The touch diagram from UV-Vis DRS measurement exhibits that the energy band gap value of pristine WO_3 nanoparticle of 2.89 eV, while for WO_3/Pt was in the range of 3.23 – 3.43 eV. PL spectra depicted the photoluminescence intensity decreasing by the addition of Pt. WO_3/Pt improved photocatalytic properties in the degradation of methylene blue (MB) under visible light for 30 min irradiation up to 98.7% degraded.

Keywords: tungsten oxide; platinum; nanoparticle; microwave assisted sol-gel; photocatalyst

1. Introduction

Water pollution is a global problem. It has been told that 14000 people die every day due to diseases caused by polluted water [1)]. The occurrence of water pollution can be caused by the presence of anthropogenic substances from textile industry waste, agricultural waste or household waste. Pollutants may consist of heavy metals, fecal bacteria, viruses, organic chemicals or dyes [2)]. The flow of waste must be treated specifically so that it can be discharged safely into the environment.

Advance Oxidation Process (AOP) is one of water treatment methods which can decompose the contaminant especially dyes in the waste water. Waste water containing dyes is one of the main environmental threats. Conventional methods such as filtration, sedimentation and absorption cannot afford to eliminate these persistent organic pollutants [3)]. Over the past few decades, waste water treatment using AOP techniques is very good for researchers because it is an advance technology that can be used to decompose very well the organic substances or toxic pollutants in the waste water [4)].

Photodegradation is one of the water treatment methods using Advance Oxidation Process technique. This method is able to decompose the dye waste into more simple components through the process of photocatalytic oxidation [5–7)]. This process produces hydroxyl radicals which will break the bound's chains of pollutant compounds so that the pollutant can be separated from the solvent. The way photodegradation works is by mixing the photocatalyst material into polluted air and by illuminating it using light. Photocatalyst materials such as Zinc oxide (ZnO), Titanium dioxide (TiO_2), Tungsten oxide (WO_3), and Cadmium sulfate (CdS) are classified as semiconductor materials with different properties and characteristics [8–11)].

Tungsten oxide (WO_3) is one of photocatalyst materials which is very promising to purify several wastes of dyestuffs such as brilliant blue, methylene blue, quasi-phenothiazine, azo, basic red 51, and trypan blue [12–18)]. Since tungsten oxide has a band gap energy value of 2.7 - 2.8 eV, it can degrade dye pollutants using visible light irradiation [19,20)].

Since the photocatalytic activity of WO_3 is still quite low in visible light, it can be increased by adding co-catalyst material such as platinum (Pt), gold (Au), or silver (Ag). In comparison to co-catalyst gold and silver, platinum is the co-catalyst that can significantly improve the photocatalytic activity of WO_3 [21)]. Widiyandari (2012) conducted a study on the effect of the addition of co-

catalyst CuO and co-catalyst platinum on the photocatalytic activity of WO_3 material and the result was both showed an increase in photocatalytic activity after the addition of co-catalyst [21]. Qamar (2011) concluded in his study that WO_3 photocatalytic activity would increase 8 times after the addition of Pt [22]. Many other studies regarding the synthesis of WO_3/Pt material as photocatalyst and the results obtained show that WO_3/Pt is optimal for applications in dye photodegradation.

WO_3 material can be synthesized through various methods such as spray pyrolysis, flame-assisted spray pyrolysis, and microwave-pyrolysis [23–25]. In previous study by using flame-assisted spray method, it produced WO_3/Pt material with a good physicochemical properties but because the procedure to manufacture WO_3/Pt is quite complicated, and it is expensive to produce WO_3/Pt [23]. As a result, in the present study, we propose a microwave-assisted sol gel method since it only requires a single step to produce the necessary material, uses a little amount of energy, and lowers the cost of manufacturing WO_3 materials. The microwave-assisted sol-gel method was also used to create WO_3/Pt photocatalyst material to enhance physicochemical and photocatalytic properties of Pt co-catalyzed WO_3 were thoroughly studied.

2. Experimental

2.1 Materials

Ammonium para tungsten ($H_{42}N_{10}O_{42}W_{12}.xH_2O$, 99%) and hexachloroplatinic acid hexahydrate ($H_2Cl_6Pt.6H_2O$, >37.5% Pt basis) were purchased from Sigma Aldrich. $HOCH_2CH_2OH$ (ethylene glycol), HNO_3 (nitric acid, 99%), and NH_3 (ammonia) were obtained from Merck. None of the all compounds were purified before usage. A Millipore system was utilized to distill and purify the water for this study.

2.2 Preparation of WO_3/Pt

The research began with the preparation of secondary solutions; platinum solution and pH stabilizer solution. A platinum solution with concentration of 10 mg/ml was prepared by dissolving 1 gram of hexachloroplatinic acid hexahydrate into 100 ml of ethylene glycol. Selection of ethylene glycol as a solvent refers to a research conducted by Zhou (2003) and Ye (2010) [25,26]. The pH stabilizer solutions were nitric acid solution (0.8 M) and ammonia solution (0.03 M). 5 mL of HNO_3 was dissolved in 100 mL of distilled water to make a nitric acid solution. Ammonia solution, on the other hand, was made by dissolving 10 mL of NH3 in 20 mL of distilled water.

Microwave-assisted sol-gel method was used to produce WO_3/Pt nanoparticles, according to previous study conducted by Ye et al., [27]. Typically, 2 grams of ammonium para tungsten was dissolved to 12 ml of distilled water under vigorous stirring and heating at 60 ℃ using a hotplate magnetic stirrer. After 10 minutes, nitric acid solution was slowly dropped gradually using a pipette to reach pH = 2.1. This mix solution was stirred and heated with a temperature of 75 ℃ and the pH was also controlled to maintain the pH value of 2.1 by dropping nitric acid solution every 30 minutes. After 4 hours, ammonia solution was dropped gradually using a pipette to reach pH = 3.5. The precursor solution was stirred and heated with a temperature of 75 ℃ for 1.5 hours and the pH was also controlled to maintain the pH value of 3.5 by dropping nitric acid solution every 30 minutes.

After those processes, platinum solution was added to the precursor solution with variations of platinum mass percentage. First, the precursor solution was transferred to a 150 ml beaker glass and then the platinum solution was dropped into the precursor solution using a measuring pipette with the appropriate volume. Second, aquadest was added with a ratio of distilled water and precursor solution of 5: 1. The precursor solution was stirred using a magnetic stirrer for 15 minutes without heating. The role of distilled water was as a medium for the microwaves when it was transmitted to the precursor solution. Then, the precursor solution was irradiated using a microwave oven with 180 W power for 10 minutes. The resulting solution would decrease in volume because of the heating process but the phase was in liquid form.

The next step was the precipitation process. The precursor solution was poured into the reaction tubes to be precipitated for 12 hours. After the precipitation, there would be two phases of matter; liquid (clear filtrate) and colloid (white sediment). The sediment would be dried through annealing process with the temperature of 600℃ for 3 hours.

2.3 Characterization of WO_3/Pt

X-ray diffractometer (XRD, Shimadzu model 6100/7000) was used to examine the crystal structure and crystal size of WO_3/Pt. Cu K radiation (λ = 0.154 nm) XRD measurements were performed at 30 kV and 30 mA with a scan step of 1° and a scan speed of 3°/min. FE-SEM observations were carried out at 15.0 kV using an JEOL model JIB-4610F to know the morphology of WO_3/Pt material and the particle size of the material. EDX (Energy Dispersive X-Ray) was connected to JIB-4610F to observe the chemical composition of WO_3/Pt material. Diffuse Reflectance UV-Vis spectrophotometer (UV 2450, Shimadzu) was used to know the value of band gap energy of WO_3/Pt material. The photoluminescence (PL) measurements using Perlin Elmer LS55, the excitation wavelength was kept at 270 nm. The PL spectra provides the information of electron-hole recombination.

2.4 Photodegradation test

Methylene blue was used as an organic dye model in this study. A 10 ppm methylene blue solution was created by combining 0.01 g of methylene blue powder with 1000 ml of aquades. The photodegradation test was carried out by irradiation of the mixture of methylene blue solution (100 ml) and WO_3/Pt photocatalyst material (0.2 g) using

sunlight simulator. To simulate sunlight conditions at AM 1.5G (100 mW/cm^2), the solar simulator (PEC-L11, Peccell Technologies, Inc., Japan) was used. After the photodegradation process was complete, the degraded solutions are separated between the filtrate and the residue using centrifuge for 15 minutes at a speed of 6000 rpm. The filtrate resulting from the separation will be calculated for its absorbance value using a UV-Vis spectrophotometer (λ= 668 nm). From the absorbance data, the concentration value of degraded methylene blue solutions could be obtained.

3. Results and discussion

3.1 WO_3/Pt material

Ammonium (para)tungstate hydrate powder ($H_{42}N_{10}O_{42}W_{12}.xH_2O$) was successfully dissolved properly into distilled water which was then added with co-catalyst platinum with a variation in the percentage of platinum mass of (0; 0.1; 0.2; 0.3; 0.4; and 0.5) wt%. The result of precursor solution has a substance phase in the form of liquid colloid with molarity of 0.05 M.

After the precursor solution was heated through annealing process, WO_3/Pt photocatalyst material was formed. The material was in the form of a yellow powder solid; bright yellow for WO_3 material without co-catalyst and brownish yellow for WO_3 material with co-catalyst platinum as shown in **Fig. 1.**

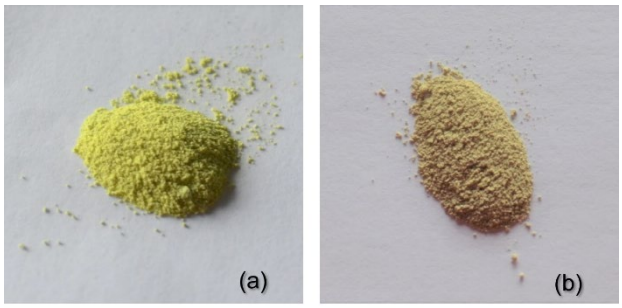

Fig. 1: WO_3/Pt material (a) WO_3 without co-catalyst (b) WO_3 with co-catalyst Pt (0.5 wt%)

3.2 Crystal structure

The diffraction pattern in **Fig. 2** shows that the variation of platinum mass percentage does not affect the position of diffraction peaks. Since there is a small percentage of platinum, the addition of co-catalyst platinum has no effect on the crystal structure of the tungsten oxide material.

When the diffraction pattern was compared with the reference data in Joint Commite on Powder Diffraction Standart (JCPDS no. 36-1451) and Match! (no. 96-101-0619), those diffraction peaks were match according to reference data. At 2θ 23.59°, 24.38°, 28.94°, 33.27°, 34.16°, 34,16°, 41,44°, 49,95°, and 56,11° the formed peaks were (020), (200), (112), (022), (202), (220), (222), (140), and (402) which are the peaks of the material of tungsten trioxide (WO_3).

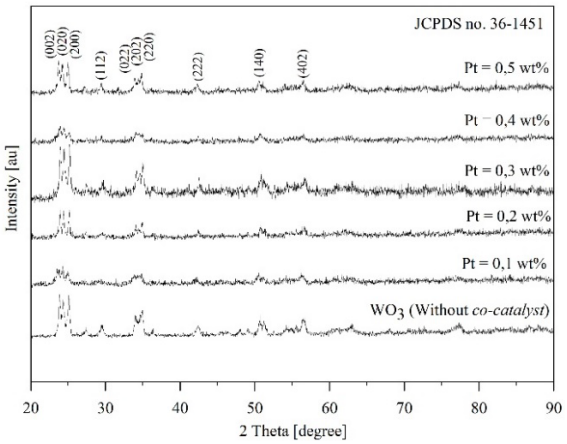

Fig. 2: Diffraction pattern of WO_3/Pt material with various percentages of platinum mass

Crystal structure of WO_3/Pt material formed for platinum mass percentage of (0; 0.1; 0.2; 0.3; 0.4; and 0.5) wt% are trichlinic (anorthic). Full Width at Half Maximum and peak angle values (2θ) obtained from XRD characterization data can be used to determine WO_3/Pt crystalline size using the Scherrer equation. The crystalline size (D_{XRD}) of WO_3/Pt material is presented in **Table 1**.

The crystallite size of the WO_3/Pt material obtained in this study ranged from 10.33 – 60.88 nm. The addition of platinum causes the crystal size to change randomly, and based on previous study, Purwanto et al., (2011) [25] was also annealing WO_3/Pt at 600ºC. WO_3/Pt produced also had random crystal size with a monoclinic structure and five dominant peaks in the diffraction plane (002), (020), (200), (112), and (002) respectively. As a result, the addition of Pt on WO_3 didn't change the cystallite size linearly.

Table 1. Crystallite size of WO_3/Pt material

Platina Mass Percentage (wt%)	D_{XRD} (nm)
0	47.90
0.1	10.33
0.2	60.88
0.3	11.14
0.4	33.32
0.5	39.38

3.3 Morphology

The FE-SEM image in **Fig. 3** shows the surface morphology of WO_3/Pt powder after annealing process. Morphology of WO_3/Pt was composed of grains with a homogeneous shape measuring about 50 nm. The formed grains agglomerated due to the WO_3/Pt powder-making process was using microwave-assisted sol-gel method.

Furthermore, the analysis of atomic composition using EDX was done to determine the presence of platinum co-catalyst in WO_3/Pt material. The peaks formed in the

graph in **Fig. 4** show the existence of the composition of the observed elements. Green peaks indicate the highest peak of each stretch of W, O and Pt that could be summarized as in **Table 2**.

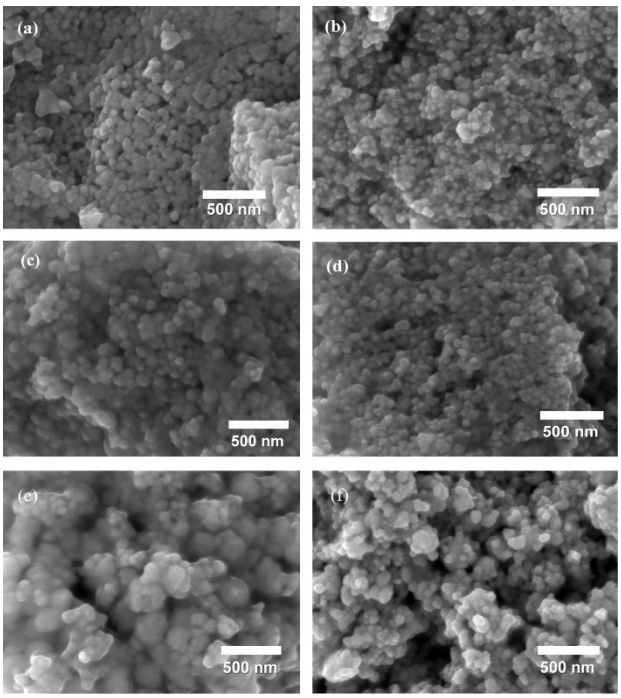

Fig. 3: FE-SEM image of WO_3/Pt with various percentages of mass Pt: (a) 0 wt%, (b) 0.1 wt%, (c) 0.2 wt%, (d) 0.3%, (e) 0.4 wt%, (f) 0.5 wt%

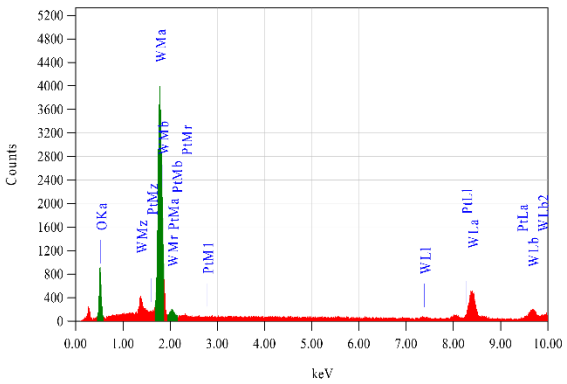

Fig. 4: EDX analysis of WO_3/Pt material (0.5 wt%)

Table 2. Chemical elements contained in WO_3/Pt material (0.5 wt%)

Element	E (keV)	Mass percentage (wt%)	Atomic percentage (at%)
O	0.525	27.82	81.60
W	1.774	70.38	17.97
Pt	2.048	1.79	0.43
Total		100.00	100.00

Table 2 summarizes the atomic composition in WO_3/Pt material. It can be seen that O atom dominated with the composition of 81.60%, while the composition of W atom was 17.97%. These values were still far if being compared with the stoichiometric value of the O and W atomic ratio in WO_3, which was 3:1. The percentage of platinum mass measured using EDX was 1.79 wt%. This value is different from the platinum mass percentage according to the stoichiometric calculations that was equal to 0.5 wt%. This is due to the uneven distribution of platinum in WO_3/Pt material so that the platinum mass percentage measured during EDX sampling was greater than its calculation.

3.4 Band gap energy

Characterization using DR UV-Vis spectrophotometer was done to calculate band gap energy values of WO_3/Pt material. Through the DR UV-Vis test, the data in the form of reflectance percentage (%R) were obtained which were then processed using Microsoft Office Excel. From the results of that data processing, the values of band gap energy through calculations using the Kubelka-Munk equation were obtained. The energy band gap values are plotted from the graph between hv (eV) vs $(hv(F(R'\infty))^{1/2}$ as shown in **Fig. 5**.

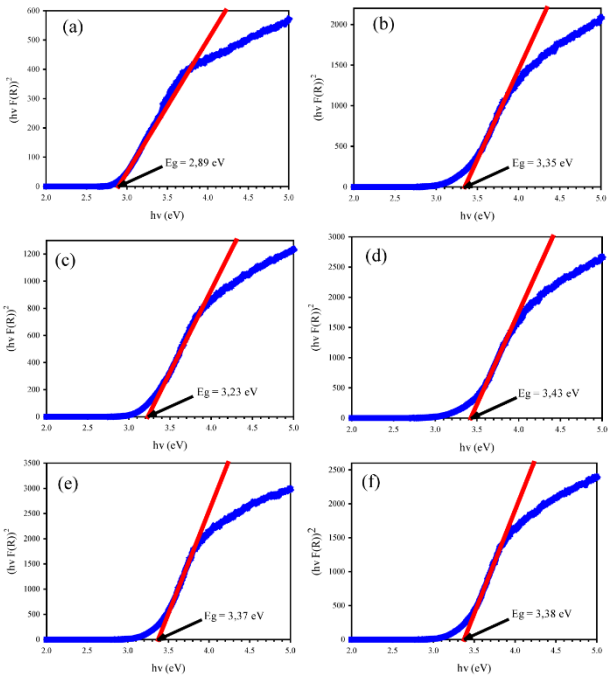

Fig. 5: Band gap energy values from WO_3/Pt material with various percentages of Pt mass, (a) 0 wt%, (b) 0.1 wt%, (c) 0.2 wt%, (d) 0.3 wt%, (e) 0.4 wt%, (f) 0.5 wt%

The band gap energy value of WO_3 material without co-catalyst in this study was 2.89 eV. This value is similar with the band gap energy value of WO_3 according to the reference that is in the range of 2.7 - 2.8 eV [19]. That value allows WO_3 material to be active in the visible light range. The addition of co-catalyst platinum to WO_3 material makes its band gap energy value larger. The band gap energy value of WO_3/Pt material in this study ranged from 3.23 – 3.43 eV. Research conducted by Shen (2015) showed that the addition of Al to the WO_3 semiconductor was shown to increase the band gap energy value to 3.22

eV after the addition of Al to the WO_3 semiconductor [26]. Aluminum and platinum have similar characteristic which are good conductor materials. It can be seen that the addition of co-catalyst material which has high electrical conductivity value on the WO_3 material can increase the value of its band gap energy.

3.5 Photoluminescence spectra

Photocatalyst electron-hole pair recombination could be caused by PL emission and to demonstrate a lower rate of recombination of electron-hole pairs, it was carried out by testing using lower PL intensities.[21]. **Fig. 6** shows the PL spectra of pure WO_3 and WO_3/Pt excited at 270 nm. It can be obviously seen that pure WO_3 nanoparticles have a high intensity emission peak of about 541 nm, and after the addition of Pt, the emission peak intensity decreases. The photoluminescence (PL) spectra of the chosen powders show a decline in PL intensity that is consistent with the WO_3 > $WO_3/Pt_{(0.3)}$ > $WO_3/Pt_{(0.1)}$ > $WO_3/Pt_{(0.2)}$ > $WO_3/Pt_{(0.5)}$ > $WO_3/Pt_{(0.4)}$. When compared to other materials, it has been found that $WO_3/Pt_{(0.4)}$ exhibits the lowest PL intensity. The results show that the Pt co-catalyst efficiently suppresses the recombination of photogenerated electron-hole pairs, and the optimal Pt addition was at 0.4 wt%. An increase in Pt (greater than 0.4 wt%) may result in surface defect locations that serve as a hub for charge carrier recombination. The separation efficiency of electron-hole pairs can be further improved by the Pt nanoparticle's capacity to serve as centers for photogenerated electron trapping.

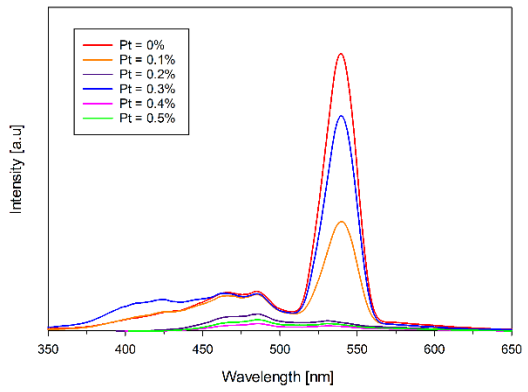

Fig. 6: Photoluminescence spectra of WO_3/Pt material with various percentages of Pt mass

3.6 Photocatalytic activity

In this study, photocatalytic activity test of WO_3/Pt (0.4 wt%) material was conducted through photodegradation test using visible light irradiation from the portable solar simulator. The dye used was a methylene blue dye. Methylene blue solution that had been mixed with photocatalyst material was irradiated using a visible light source of 1000 W/m^2 for 30 minutes. This test was conducted to determine the effect of adding co-catalyst platinum to photocatalytic activity of WO_3 material. Photodegradation test was done in three conditions: methylene blue solution without photocatalyst, methylene blue solution with WO_3 photocatalyst and methylene blue solution with WO_3/Pt (0.4 wt%) photocatalyst. An UV-vis spectrophotometer was used to measure the absorbance of degraded methylene blue solutions. From the absorbance data, the concentration value of degraded methylene blue solutions could be obtained (calculated using calibration curve of methylene blue solution) (presented in **Fig. 7.a).**

The Digital photo of the samples, before and after the photodegradation test are shown in **Fig. 7.b.** Methylene blue solution that was degraded without photocatalyst addition did not experience a significant color change when observed visually. However, when viewed from its concentration value (**Fig. 7.a**), the solution of methylene blue which originally had a concentration value of 10 ppm decreased to 5.101 ppm. This shows that even without photocatalyst material a solution of methylene blue could also be degraded when irradiated using visible light. It can be concluded that a photolysis process occurred between dyes and light from solar simulators, which also played a role in the degradation process.

The color changes of the methylene blue solution indicated the photodegradation success rate (clearer than before). The results obtained from the photodegradation test showed that pristine WO_3 and WO_3/Pt (0.4 wt%) which were synthesized using microwave-assisted sol-gel method both of them were able to degrade 10 ppm methylene blue dye under visible light well. The degradation could be seen from the physical changes in the methylene blue solutions, which were originally blue to clear.

The addition of co-catalyst platinum had been shown to increase the photocatalytic activity of WO_3. Degradation with WO_3 material produced a methylene blue solution with a concentration of 0.675 ppm, whereas degradation with WO_3/Pt (0.4 wt%) produced a methylene blue solution with a concentration of 0.217 ppm.

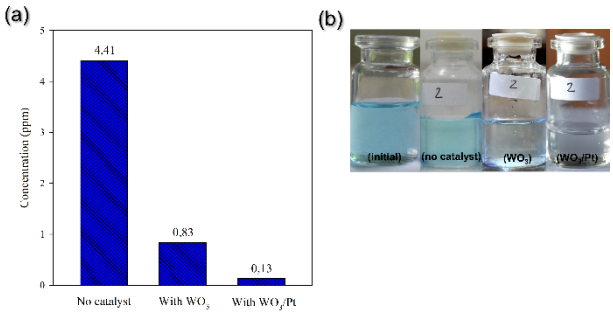

Fig. 7: (a) Concentation of methylene blue solution after photodegradation for 30 min, (b) Digital photo of the samples before and after photodegradation test

4. Conclusions

Tungsten oxide with co-catalyst Pt (WO_3/Pt) was successfully synthesized using the microwave-assisted sol-gel method with variations in platinum mass percentage of (0; 0.1; 0.2; 0.3; 0.4; and 0.5) wt%.The

results show that, the band gap energy of WO_3 without co-catalyst was 2.89 eV and for WO_3 with platinum co-catalyst (WO_3/Pt) was increasing the band energy of WO_3 in the range of 3.23 – 3.43 eV. The process of adding a platinum co-catalyst with a mass percentage of 0.1 wt% – 0.5 wt% into the WO_3 material did not significantly affect the crystallinity or morphology of the WO_3 material. However, tungsten oxide with Pt co-catalyst was found to have better photocatalytic activity than tungsten oxide without co-catalyst.

Acknowledgements

This author acknowledges the Ministry of Education, Culture, Research, and Technology, Republic of Indonesia, under the grant of world-class research (WCR) for funding this research with contract number: 821/UN27/KP/2019 and 2104/UN27.22/PT.01.03/2021. The authors (HW, WBW) acknowledge Research Center for Physics, Indonesian Institute of Sciences for providing microscopy analyses in this research.

References

1) UNICEF, and WHO, "Lack of sanitation for 2.4 billion people is undermining health improvements," *WHO/UNICEF News Release*, (2015).
2) T. Munawar, S. Yasmeen, M. Hasan, K. Mahmood, A. Hussain, A. Ali, M.I. Arshad, and F. Iqbal, "Novel tri-phase heterostructured ZnO–$Yb2O_3$–$Pr2O_3$ nanocomposite; structural, optical, photocatalytic and antibacterial studies," *Ceram. Int.*, **46** (*8*) 11101–11114 (2020). doi:10.1016/j.ceramint.2020.01.130.
3) P. V. Nidheesh, M. Zhou, and M.A. Oturan, "An overview on the removal of synthetic dyes from water by electrochemical advanced oxidation processes," *Chemosphere*, **197** 210-227 (2018). doi:10.1016/j.chemosphere.2017.12.195.
4) B. Bethi, S.H. Sonawane, B.A. Bhanvase, and S.P. Gumfekar, "Nanomaterials-based advanced oxidation processes for wastewater treatment: a review," *Chem. Eng. Process. Process Intensif.*, **109** 178-189 (2016). doi:10.1016/j.cep.2016.08.016.
5) B. Pant, H.R. Pant, N.A.M. Barakat, M. Park, K. Jeon, Y. Choi, and H.Y. Kim, "Carbon nanofibers decorated with binary semiconductor (TiO_2/ZnO) nanocomposites for the effective removal of organic pollutants and the enhancement of antibacterial activities," *Ceram. Int.*, **39** (*6*) 7029–7035 (2013). doi:10.1016/j.ceramint.2013.02.041.
6) N.I.I. Zamri, S.L.N. Zulmajdi, E. Kusrini, K. Ayuningtyas, H.M. Yasin, and A. Usman, "Rhodamine b photocatalytic degradation using CuO particles under uv light irradiation for applications in industrial and medical fields," *Evergreen*, **7** (*2*) 280–284 (2020). doi:10.5109/4055233.
7) A. Azani, D.S.C. Halin, M.M. Al Bakri Abdullah, K.A. Razak, M.F.S.A. Razak, M.M. din Ramli, M.A.A.M. Salleh, and V. Chobpattana, "The effect of go/tio2 thin film during photodegradation of methylene blue dye," *Evergreen*, **8** (*3*) 556–564 (2021). doi:10.5109/4491643.
8) O. Carp, C.L. Huisman, and A. Reller, "Photoinduced reactivity of titanium dioxide," *Prog. Solid State Chem.*, **32** (*1–2*) 33-177 (2004). doi:10.1016/j.progsolidstchem.2004.08.001.
9) H. Iwakura, H. Einaga, and Y. Teraoka, "Photocatalytic properties of ordered double perovskite oxides," *Kyushu Univ. Glob. COE Progr. J. Nov. Carbon Resour. Sci.*, **3** 1–5 (2011).
10) I.H. Dwirekso, M. Ibadurrohman, and Slamet, "Synthesis of tio2-sio2-cuo nanocomposite material and its activities for self-cleaning," *Evergreen*, **7** (*2*) 285–291 (2020). doi:10.5109/4055234.
11) K. Taira, and H. Einaga, "Distribution ratio of pt on anatase and rutile tio2 particles, determined by x-ray diffraction and transmission electron microscopy analysis of pt/tio2(p25)," *Evergreen*, **5** (*4*) 13–17 (2018). doi:10.5109/2174853.
12) Y.M. Hunge, A.A. Yadav, and V.L. Mathe, "Ultrasound assisted synthesis of WO_3-ZnO nanocomposites for brilliant blue dye degradation," *Ultrason. Sonochem.*, **45** 116-122 (2018). doi:10.1016/j.ultsonch.2018.02.052.
13) L. Gan, L. Xu, S. Shang, X. Zhou, and L. Meng, "Visible light induced methylene blue dye degradation photo-catalyzed by WO_3/graphene nanocomposites and the mechanism," *Ceram. Int.*, **42** (*14*) 15235-15241 (2016). doi:10.1016/j.ceramint.2016.06.160.
14) H. Wang, C. Wang, X. Cui, L. Qin, R. Ding, L. Wang, Z. Liu, Z. Zheng, and B. Lv, "Design and facile one-step synthesis of $FeWO_4$/Fe_2O_3 di-modified WO_3 with super high photocatalytic activity toward degradation of quasi-phenothiazine dyes," *Appl. Catal. B Environ.*, **221** 169-178 (2018). doi:10.1016/j.apcatb.2017.09.011.
15) S. V. Mohite, V. V. Ganbavle, and K.Y. Rajpure, "Photoelectrocatalytic activity of immobilized yb doped WO_3 photocatalyst for degradation of methyl orange dye," *J. Energy Chem.*, **26** (*3*) 440-447 (2017). doi:10.1016/j.jechem.2017.01.001.
16) R. Malik, P.S. Rana, V.K. Tomer, V. Chaudhary, S.P. Nehra, and S. Duhan, "Nano gold supported on ordered mesoporous wo3/sba-15 hybrid nanocomposite for oxidative decolorization of azo dye," *Microporous Mesoporous Mater.*, **225** 245-254 (2016). doi:10.1016/j.micromeso.2015.12.013.
17) L.E. Fraga, J.H. Franco, M.O. Orlandi, and M.V.B. Zanoni, "Photoelectrocatalytic oxidation of hair dye basic red 51 at W/WO_3/TiO_2 bicomposite photoanode activated by ultraviolet and visible radiation," *J. Environ. Chem. Eng.*, **1** (*3*) 194-199 (2013). doi:10.1016/j.jece.2013.04.018.

18) A.N. Subba Rao, V.T. Venkatarangaiah, G.B. Nagarajappa, S.H. Nataraj, and P.M. Krishnegowda, "Enhancement in the photo-electrocatalytic activity of sno2-sb2o4 mixed metal oxide anode by nano-wo3 modification: application to trypan blue dye degradation," *J. Environ. Chem. Eng.*, **5** (*5*) 4969-4979 (2017). doi:10.1016/j.jece.2017.09.033.
19) W. Morales, M. Cason, O. Aina, N.R. De Tacconi, and K. Rajeshwar, "Combustion synthesis and characterization of nanocrystalline WO_3," *J. Am. Chem. Soc.*, **130** (*20*) 6318–6319 (2008). doi:10.1021/ja8012402.
20) M. Ezaki, and K. Kusakabe, "Highly crystallized tungsten trioxide loaded titania composites prepared by using ionic liquids and their photocatalytic behaviors highly crystallized tungsten trioxide loaded titania composites prepared by using ionic liquids and their photocatalytic beh," *Evergreen*, **1** (*2*) 18–24 (2014).
21) H. Widiyandari, A. Purwanto, R. Balgis, T. Ogi, and K. Okuyama, "CuO/wo 3 and pt/wo 3 nanocatalysts for efficient pollutant degradation using visible light irradiation," *Chem. Eng. J.*, **180** 323–329 (2012). doi:10.1016/j.cej.2011.10.095.
22) M. Qamar, Z.H. Yamani, M.A. Gondal, and K. Alhooshani, "Synthesis and comparative photocatalytic activity of Pt/WO_3 and Au/WO_3 nanocomposites under sunlight-type excitation," *Solid State Sci.*, **13** (*9*) 1748-1754 (2011). doi:10.1016/j.solidstatesciences.2011.07.002.
23) O. Arutanti, A.B.D. Nandiyanto, T. Ogi, F. Iskandar, T.O. Kim, and K. Okuyama, "Synthesis of composite WO_3/TiO_2 nanoparticles by flame-assisted spray pyrolysis and their photocatalytic activity," *J. Alloys Compd.*, **591** 121-126 (2014). doi:10.1016/j.jallcom.2013.12.218.
24) A.B.D. Nandiyanto, O. Arutanti, T. Ogi, F. Iskandar, T.O. Kim, and K. Okuyama, "Synthesis of spherical macroporous WO_3 particles and their high photocatalytic performance," *Chem. Eng. Sci.*, **101** 523-532 (2013). doi:10.1016/j.ces.2013.06.049.
25) A. Purwanto, H. Widiyandari, T. Ogi, and K. Okuyama, "Role of particle size for platinum-loaded tungsten oxide nanoparticles during dye photodegradation under solar-simulated irradiation," *Catal. Commun.*, **12** (*6*) 525-529 (2011). doi:10.1016/j.catcom.2010.11.020.
26) Y. Shen, P. Yan, Y. Yang, F. Hu, Y. Xiao, L. Pan, and Z. Li, "Hydrothermal synthesis and studies on photochromic properties of al doped WO_3 powder," *J. Alloys Compd.*, **629** 27-31 (2015). doi:10.1016/j.jallcom.2014.11.218.
27) J. Ye, J. Liu, Z. Zou, J. Gu, and T. Yu, "Preparation of Pt supported on WO_3-C with enhanced catalytic activity by microwave-pyrolysis method," *J. Power Sources*, **195** (*9*) 2633-2637 (2010). doi:10.1016/j.jpowsour.2009.11.055.